Journal of Chromatography, 465 (1989) 137–156
Elsevier Science Publishers B.V., Amsterdam — Printed in The Netherlands

CHROM. 21 148

ION-EXCHANGE EQUILIBRIA OF LYSOZYME, MYOGLOBIN AND BOVINE SERUM ALBUMIN

EFFECTIVE VALENCE AND EXCHANGER CAPACITY

R. D. WHITLEY, R. WACHTER, F. LIU and N.-H. L. WANG*
School of Chemical Engineering, Purdue University, West Lafayette, IN 47906 (U.S.A.)
(First received September 15th, 1988; revised manuscript received November 29th, 1988)

SUMMARY

A series of ion-exchange equilibrium experiments were completed and analyzed by a mass action model. The isotherms at various counter-ion concentrations are regressed to determine the average number of binding sites, Z, the mass action constant, K, and the effective capacity of the exchanger, P_m. The estimates for P_m are 1–10 mmol of protein adsorbed per liter of packed Sepharose exchanger, in agreement with values determined from fitting the Langmuir isotherms. A geometric model, developed to relate the charge distribution of the exchanger and the size of the protein to the protein capacity, also confirms the estimates of P_m.

The Z values estimated (and confirmed with an independent slope method) range from 0.8 to 3.6, indicating that most of the ionized sites on the protein do not undergo ion exchange. Geometric model estimates of exchanger sites covered by a protein at maximum surface coverage show that only 1–32% of the sites actually undergo ion exchange. This result indicates that adsorbed protein molecules "block" many exchanger sites, preventing other molecules from ion exchanging at those sites. This high degree of blocking by proteins also indicates that there is an excess of exchanger sites, as evidenced by Z showing no dependence on charge separation distance over the range 6–10 Å.

Scatchard pots of the equilibrium data indicate that there is competition between at least two different binding forms of each protein studied. For the high-affinity systems, cooperative binding was observed at low exchanger loading; the character then changed to heterogeneous competitive binding as the exchanger loading increased. The effect on an isotherm plot is a subtle but systematic deviation from the Langmuir and mass action models. More important, the competition means that Z represents an average for competing binding forms and, as such, Z can be fractional.

INTRODUCTION

The separation of proteins by ion exchange usually requires changes in pH and salt (counter-ion) concentration. These changes affect the three-dimensional struc-

0021-9673/89/$03.50

tures and charge distributions of the proteins, shifting protein affinity in ways which are difficult to predict. The type of exchanger, its charge density and structural characteristics can have equally profound effects on the separation. A model that could accurately account for all of these effects would be extremely complex and would require extensive information about the system.

What would be more reasonable is a model that requires a moderate amount of system information, yet still gives useful predictions of behavior for a wide range of conditions. In this research we have developed a mass action model which closely describes the ion exchange of proteins using only three fitted parameters (average binding number, Z, protein capacity of the exchanger, P_m, and equilibrium parameter, K). The regressed Z values are compared with those determined by a slope method[1]. Myoglobin, lysozyme and bovine serum albumin all have known amino acid sequences, allowing us to determine the maximum number of charge sites available for binding.

To gain a better understanding of the physical interaction of the protein molecules with the exchangers, we have developed a geometric model for the interaction of charged surfaces. This model also allows comparison between the regressed value of protein capacity for the exchanger and the expected value based solely on geometric considerations. The exchangers (CM-, DEAE-, Q- and S-Sepharose) were selected to provide a range of surface charge densities for the geometric model.

Competition of various binding forms was explored by Scatchard plots. The proposed model is also compared with another mass action model, proposed by Mazsaroff *et al.*[2], that requires five fitted parameters and provides a sigmoidal dependence of Z on adsorbed protein concentration.

THEORY

The basic principles of ion exchange were discussed by Walton[3]. However, most of the cases considered were limited to small, inorganic ions. The basic ion-exchange relationship for this type of batch equilibrium experiment was used by Boardman and Partridge[1] in a study of proteins. It was also derived in terms of a mass action expression by Velayudhan and Horváth[4]. The idea has also been presented in a series of papers by Regnier's group[5–7]. In general terms, the ion-exchange process may be represented by the following "reaction":

$$P + ZC_b \leftrightharpoons P_b + ZC \tag{1}$$

where P and P_b are protein concentrations in the liquid and solid phases, respectively, and C and C_b are the analogs for the counter ion; Z represents the average number of binding sites between a protein molecule and the exchanger. For our experimental conditions we used only monovalent salts in order to focus on the behavior of the protein binding.

The model assumes that the ion-exchange process can be approximated by a single adsorption step with a constant number of binding sites (independent of concentration). From this "reaction" one obtains the following equilibrium expression (defining a binary selectivity coefficient in terms of concentrations):

$$K_b = \frac{P_b C^Z}{P C_b^Z} \tag{2}$$

Next, an empirical parameter, K_f is introduced to account for the fraction of charges on the exchanger that are actually accessible to the bulky protein molecule:

$$C_b = K_f q_m - Z P_b \tag{3}$$

Here C_b is actually the total concentration of counter ion that is accessible to the protein and q_m is the small ion-capacity of the exchanger in mN. This equation can be rearranged in terms of the protein capacity of the exchanger, $[P_m]$, in units of mM;

$$C_b = Z(P_m - P_b) \tag{4}$$

where $P_m = K_f q_m / Z$, representing the maximum number of moles of protein which can be bound to the exchanger. Substituting this expression into eqn. 2 and solving for P_b, one obtains

$$P_b = K_b Z^Z P \left(\frac{P_m - P_b}{C} \right)^Z \tag{5}$$

Combining constant terms gives

$$P_b = KP \left(\frac{P_m - P_b}{C} \right)^Z \tag{6}$$

where

$$K = K_b Z^Z \tag{7}$$

and C is approximately equal to C_0, the initial counter-ion concentration in free solution, as the free solution volume is much greater than the exchanger volume under our experimental conditions. If Z is set equal to 1, the mass action expression may be rearranged to form a Langmuir expression:

$$P_b = \frac{aP}{1 + bP} \tag{8}$$

where

$$a = \frac{KP_m}{C} \tag{9}$$

and

$$b = \frac{K}{C} \tag{10}$$

The mass action model represents an isotherm over varying counter-ion levels for a specific pH. A similar model has been applied to the high-performance ion-exchange chromatography of proteins by Kopaciewicz *et al.*[5] for very low surface coverage. Additional column evaluation of the model was presented by Rounds and Regnier[6]. The limitations of applying this model to proteins have been discussed elsewhere[8].

Determination of ion-exchange capacity

The ion-exchange capacity per unit volume must be determined experimentally for each system. The exchange capacity is affected by the type and porosity of the exchanger, charge density and charge distribution on the sorbents. As each solute usually differs in size, shape and charge distribution, it will have access to a unique fraction of the binding sites. For a binary exchange system, competition occurs at the exchanger sites which are accessible to both compounds. For our experimental conditions, the species in competition are Cl^- or Na^+ and a protein. From size considerations alone, a given exchanger will have a smaller capacity for a protein than for an inorganic ion. We denote this protein capacity as P_m in terms of millimoles of protein per liter of packed exchanger.

Determination of apparent binding number

One complexity of protein ion exchage arises from the different ways in which an individual protein molecule may bind to an exchanger. This competition among various binding forms causes a change in the apparent (average) Z as a function of protein concentration[8]. The mass action model discussed in this paper assumes that the equilibrium behavior can be represented by an average Z value for the conditions of interest. Other researchers[2] have proposed an empirical model to describe the variation of Z with bound protein concentration. The merits of both methods will be discussed later.

The value of Z at low surface coverage can be estimated by a slope method. We begin with eqn. 6, written for low surface coverage (C approximately constant at the initial value, C_0, and $P_m - P_b$ approximately equal to the exchanger capacity, P_m):

$$P_b = KP\left(\frac{P_m}{C_0}\right)^z \tag{11}$$

Taking logarithms and rearranging gives

$$\log\left(\frac{P_b}{P}\right) = \log K + Z \log\left(\frac{P_m}{C_0}\right) \tag{12}$$

If the P_b *versus* P data are fitted to a Langmuir isotherm (eqn. 8), the Langmuir

coefficient, a, at low surface coverage is equivalent to the P_b/P term in eqn. 12. Plotting log a *versus* log (P_m/C_0) then gives Z as the slope. This relationship serves as a check of the Z values from the mass action model in the limiting case of low surface coverage.

Numerical techniques

The non-linear least-squares regression was performed on eqn. 6 as part of a Fortran program; the data consisted of $P_b = f(P,C_0)$. The IMSL (International Mathematical and Statistical Libraries, edition 10, Houston, TX, U.S.A.) routine DUNLSF uses a finite difference, Levenberg–Marquardt algorithm (using strict descent) to fit Z, K and P_m. After convergence, fitted values of P_b were calculated by the IMSL routine ZBREN, which uses a combination of linear interpolation, inverse quadratic interpolation and bisection and usually gives better than linear convergence.

To aid in quantifying the accuracy of the parameter estimations, a computer program was developed to examine the sum of squares of error for perturbations in any two of the three regressed parameters for a constant value of the third parameter. This program reads the regressed estimates and generates a grid of perturbed estimates of two of the parameters within a given percentage. The sum of squares of error $(P_b - \hat{P}_b)$, SSE, is determined for each of these grid points. The contouring package of DI3000 (Precision Visuals, Boulder, CO, U.S.A.) then uses that information to generate the constant-error curves for the particular data set. Departure of the orientation of the oval error curves from parallel to the axes gives a measure of parameter correlation. As the parameters become more correlated, the individual confidence intervals have less meaning and combined intervals should be used.

EXPERIMENTAL

Materials

The ion exchangers used, Q-Sepharose Fast Flow (strong anion), DEAE-Sepharose Fast Flow (weak anion), S-Sepharose Fast Flow (strong cation), CM-Sepharose Fast Flow (weak cation), were purchased from Pharmacia (Uppsala, Sweden). Sepharose ion exchangers are composed of agarose, a macroporous gel with good stability. The three different proteins used for the study [bovine serum albumin (BSA), horse heart myoglobin (MYO) and lysozyme (LYO)] were purchased from Sigma (St. Louis, MO, U.S.A.). The properties of these ion exchangers and proteins are given in Table I and Table II, respectively. The experimental conditions are

TABLE I
TOTAL SMALL ION CAPACITIES

Ion exchanger	*pH*	*Capacity (μequiv./ml)*
DEAE-Sepharose FF	6.0	112
	8.0	84
Q-Sepharose FF	6.0	210
	8.0	210
CM-Sepharose FF	4.0	55
	5.0	99
S-Sepharose FF	4.0	210
	5.0	210

TABLE II
PROPERTIES OF SELECTED PROTEINS

Protein	*MW*	*pI*[a]	*Residues*	*Size (Å)*
BSA	67 000	4.98, 5.07, 5.18	582	141 × 42
MYO	17 500	6.9, 7.3	153	45 × 35 × 25
LYO	13 930	11.0	129	45 × 30 × 30

[a] Isoelectric points from Righetti and Caravaggio[18].

abbreviated using the convention protein/exchanger/pH, *e.g.*, MYO/CM/5 refers to myoglobin on CM-Sepharose Fast Flow at pH 5.

To avoid problems associated with a counter ion with multiple binding sites, the counter ion selected for all experiments was singly charged. Tris(hydroxymethyl)-aminomethane (Tris) and bis(2-hydroxyethyl)iminotris(hydroxymethyl)methane (Bis-Tris) buffers were selected for the anion exchangers, while the acetate buffer was used for the cation exchange system. The buffers were purchased from Sigma.

Batch experiments

Because proteins can be denatured at the air–liquid interface, foaming and aeration of the solutions were minimized. The buffer concentration for all of the experiments was 0.1 *M*, sufficient to maintain a constant pH over the concentration range studied. Before an exchanger was used, it was loaded with the counter ion of the experiment. The exchanger was then equilibrated by washing with six aliquots of a buffered salt solution under experimental conditions as suggested by Pharmacia[9].

A series of concentrations of protein solution was selected for each isotherm. For each concentration, a test-tube was filled with 5 ml of the buffered protein solution and 1 ml of the exchanger suspension (yielding about a 0.3-ml packed bed volume of exchanger). The tubes were gently rotated end-over-end for 25 h at 25°C, then the UV absorbance was measured at 280 nm. The exchangers have a particle void volume of 95%, making quantification by dry weight difficult (the degree of drying is not reproducible). We therefore selected the packed bed volume as the best measure to represent the amount of exchanger. This volume is determined by taking the exchanger from a test-tube after equilibration and packing it into a small, graduated column. The volume of packed exchanger is read, while the column is wetted, to a precision of ± 0.05 ml. The accuracy of this measurement was in line with that of other measurements in the experiments.

RESULTS AND DISCUSSION

Experimental isotherms

The resulting isotherms appear in Figs. 1–8. The best-fit curves are from the Langmuir model applied at each salt concentration. Each isotherm was regressed to obtain the Langmuir coefficients and their 95% confidence intervals (Table III). The Langmuir model fits the individual isotherms fairly well but does not allow for the dependence on salt concentration.

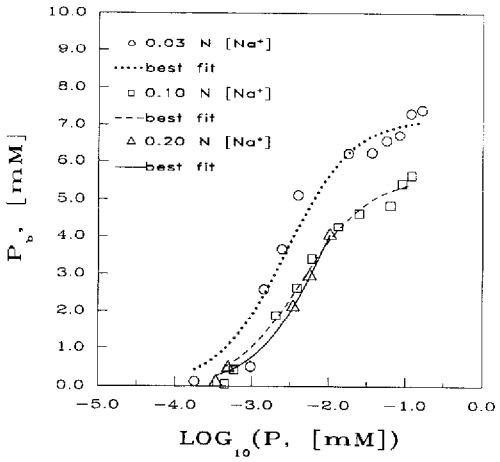

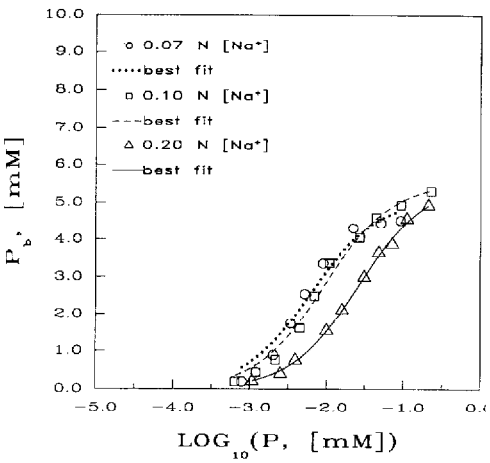

Fig. 1. Equilibrium binding isotherms for myoglobin on CM-Sepharose Fast Flow at pH 4.

Fig. 2. Equilibrium binding isotherms for myoglobin on CM-Sepharose Fast Flow at pH 5.

The independent axis was plotted as log P in order to expand the low-concentration region. Some general trends can be noted immediately. Most of the curves show an elongated "S" shape as a result of the logarithmic scaling. In most instances the isotherms show at least the beginnings of monolayer saturation, which is indicated by the decrease in slope at higher P. The protein concentrations for these isotherms are well below saturation of the small ion capacities, indicating that, at most, 32% of the total exchanger capacity is used by the proteins.

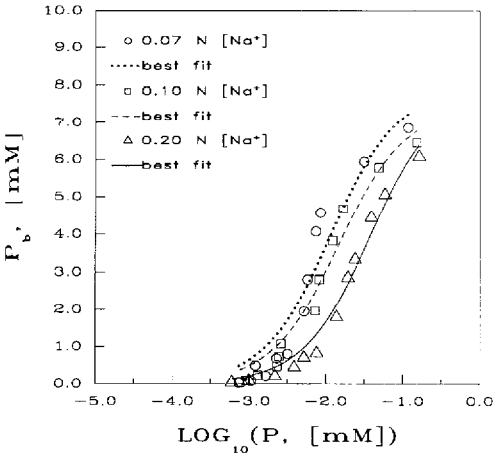

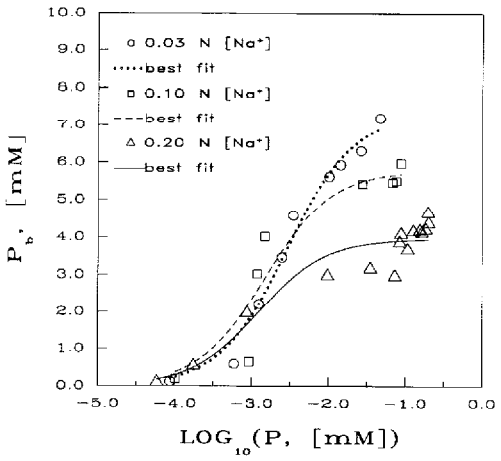

Fig. 3. Equilibrium binding isotherms for myoglobin on S-Sepharose Fast Flow at pH 5.

Fig. 4. Equilibrium binding isotherms for lysozyme on CM-Sepharose Fast Flow at pH 4.

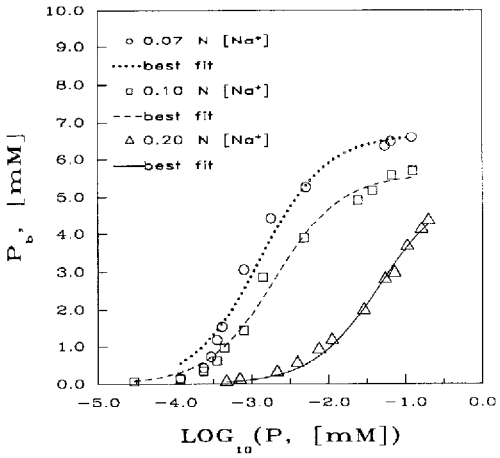

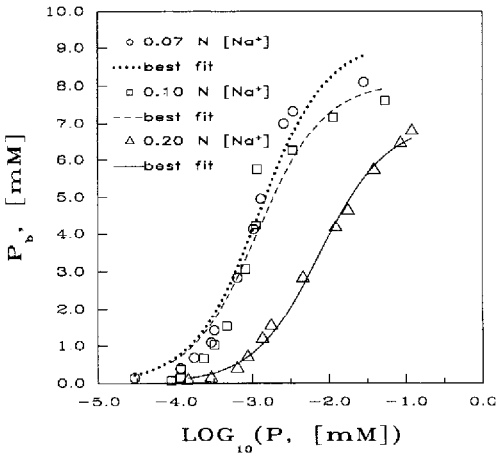

Fig. 5. Equilibrium binding isotherms for lysozyme on CM-Sepharose Fast Flow at pH 5.

Fig. 6. Equilibrium binding isotherms for lysozyme on S-Sepharose Fast Flow at pH 5.

Determination of mass action model parameters

Before applying the model to batch data at different salt concentrations, we conducted a series of tests with four synthetic isotherms. These tests served both as a check on the program and as a gage of the model characteristics. The isotherms have $Z = 4$, $K = 1280$, $P_m = 21$ mM, $C_0 = 80$, 100, 150 and 200 mM, and a range of P values (0–1.5 mM). The first check was on the Z, K and P_m regression program. Runs on the four test sets returned $Z = 4$, $K = 1280$ and $P_m = 21$ mM for a wide series of initial guesses, and within the round-off error, had zero standard deviation.

In eqn. 6, if P_m is much greater than P_b, the model will predict a linear isotherm.

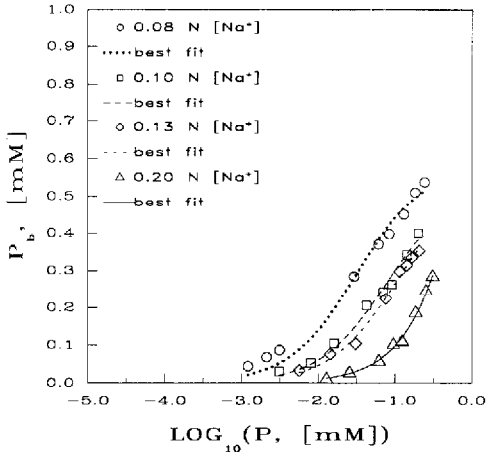

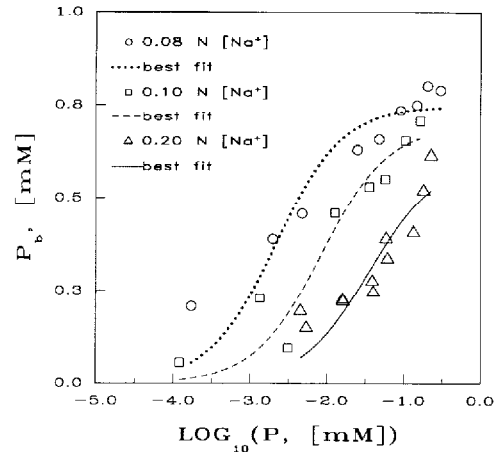

Fig. 7. Equilibrium binding isotherms for bovine serum albumin on DEAE-Sepharose Fast Flow at pH 8.

Fig. 8. Equilibrium binding isotherms for bovine serum albumin on Q-Sepharose Fast Flow at pH 8.

TABLE III
LANGMUIR COEFFICIENTS

Conditions[a]	$C_0(mM)$	a	$b(mM^{-1})$	$a/b(mM)$
MYO/CM/4	30.0	2581	358.7	7.19
	100.0	1256	224.6	5.59
	200.0	843.9	112.2	7.52
MYO/CM/5	70.0	811.4	158.5	5.12
	100.0	588.5	106.3	5.54
	200.0	209.9	37.9	5.53
MYO/SS/5	70.0	692.8	87.3	7.93
	100.0	510.9	68.9	7.42
	200.0	211.9	27.0	7.85
LYO/CM/4	30.0	2585	353.8	7.31
	100.0	3948	683.9	5.77
	200.0	3265	825.7	3.95
LYO/CM/5	70.0	5214	785.0	6.64
	100.0	2804	501.4	5.59
	200.0	114.0	21.9	5.21
LYO/SS/5	70.0	7311	795.6	9.19
	100.0	6820	841.9	8.10
	200.0	902.2	129.2	6.98
BSA/DS/8	80.0	18.4	31.7	0.58
	100.0	6.81	12.8	0.53
	130.0	5.05	9.18	0.55
	200.0	1.00	0.23	4.32
BSA/QS/8	80.0	345.5	462.3	0.75
	100.0	81.4	117.4	0.69
	200.0	16.8	28.0	0.60

[a] Protein/exchanger/pH.

This is indeed what happens if the small ion capacity is used. Clearly, most of the isotherms in Figs. 1–8 show distinct curvature. For this reason and the molecule size consideration discussed earlier, P_m must be a fitted parameter, specific for a particular protein–exchanger combination.

Once the parameters had been determined, we wished to judge the resulting behavior of the model. As the plot of $P_b = f(P,C_0)$ is three-dimensional, we also wanted to check visually for any patterns in the difference between the data and the model prediction. In Fig. 9 the BSA/DS/8 isotherms are shown with the model surface. The vertical lines emanating from the data points represent the differences between the model estimates and the actual data points. The lower C_0 isotherms have fairly steep curvature at low P. This behavior cannot be well accommodated by the model and is probably due to a change in the value of Z as an inverse function of P. Fig. 10 shows this comparison for the MYO/CM/5 isotherms (three C_0 levels). Here, too, the initial slope is underestimated. Myoglobin binds fairly readily to the cation exchanger, so the initial slope is steep.

The characteristic curvature of the isotherms (constant C_0 in the three-dimensional plots) was not given by the model when the small ion capacities were used in the fit; it predicted a higher value of P_b for saturation. Using the lower, fitted values for P_m gives the expected curvature and a reduced standard deviation, indicating that

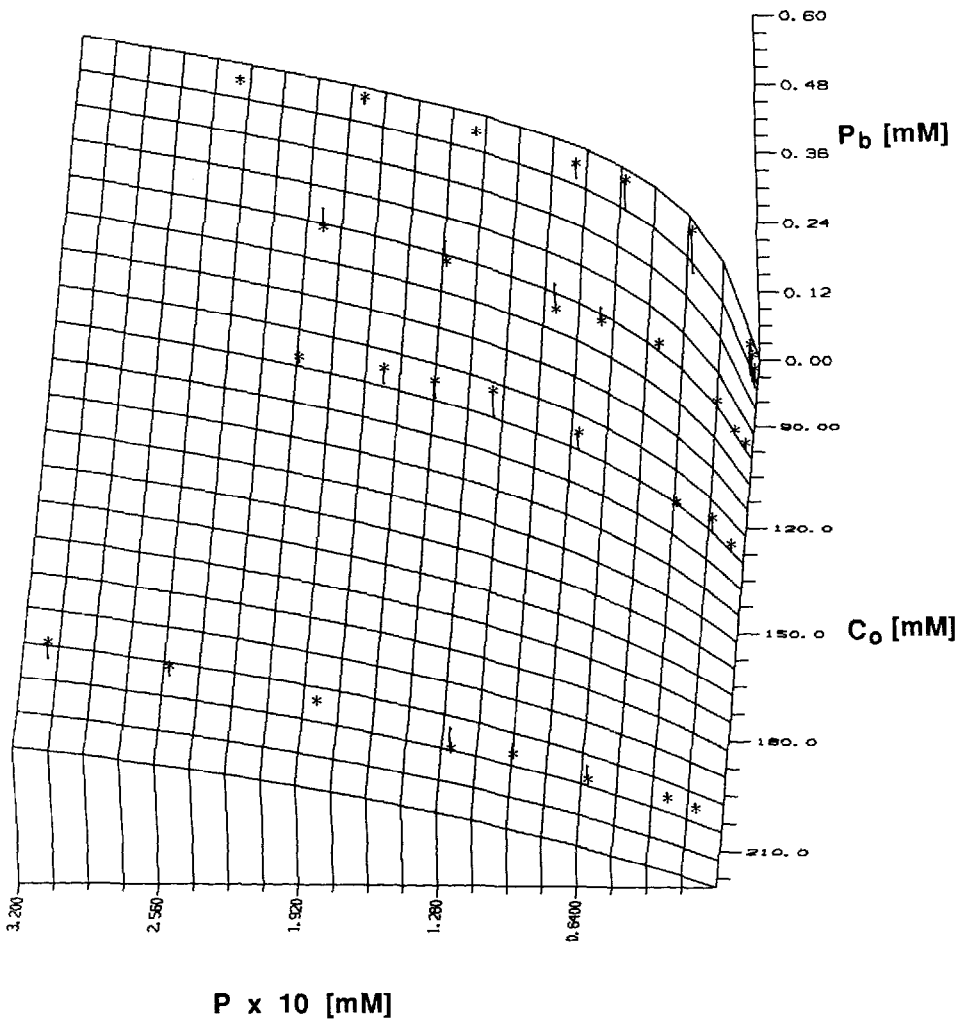

Fig. 9. Comparison of mass action model with batch data for BSA/DS/8. The vertical lines represent difference between model and data values of P_b.

a much lower value for saturation is justified. In general, with P_m fitted from the data, the curvature in the model isotherm still cannot match that of the data isotherm for the range of salt levels investigated. For all three C_0 levels in Fig. 10, the slope at the beginning and end of the isotherms is underestimated and overestimated, respectively. This behavior can be described by an initially high value of Z, decreasing as surface coverage increases. This inverse dependence of Z on protein concentration concurs with the behavior of basic amino acids reported by Wang *et al.*[10]. They studied cation exchange of basic amino acids which had two types of binding: monovalent binding at the side-chain amino group and divalent binding at both the α and side-chain amino groups. At a given pH and salt concentration, the average Z decreased from 2 to 1 with

increase in amino acid concentration. As proteins have numerous binding groups and potentially heterogeneous binding, similar behavior may be expected. This trait will be examined in more detail later.

Table IV shows the Z, K and P_m values for the sets of experiments. Confidence intervals for this model were determined by ignoring the correlation between the parameters beyond the first derivative (linear approximation). The approximate 95% confidence intervals are included in Table IV. The wide confidence interval for K indicates that there may be some correlation between the parameters. Correlations can be readily visualized by a contour analysis of the model. For the best parameter estimates, the SSE between the model and the data is minimized. Taking slightly perturbed values of any two parameters (keeping all others constant) will increase the SSE in a smooth manner. Connecting all points of equal SSE around the minimum will generate a series of contours. The shape of the contours and their orientation relative to the axes indicates the degrees of scaling problems and correlation, respectively. Perfectly circular contours indicate no correlation and perfect scaling. If the contours are elongated, correlation is indicated by orientation of the oval away from alignment with the axes. Scaling problems make the parameter search more difficult, but correlation between parameters renders individual confidence intervals less useful (one should consider combined confidence surfaces)[11].

The confidence level for the parameter estimates is related to the constant SSE curves by the F statistic[11]:

$$S_c = S_{min} + s^2_{pool} n F_{0.05}(n,m) \tag{13}$$

where S_c is the sum of squares for the contour, S_{min} is the minimum sum of squares (for the best-fit of parameters), s^2_{pool} is the pooled variance of the data sets, n is the number of parameters being estimated, F is the F statistic and m is the degrees of freedom (number of points minus n). All of the contour plots for K *versus* Z perturbations, including the test data set, showed ovals greatly elongated parallel to the K axis and oriented slightly clockwise (Fig. 11). Hence K could be scaled better, and the degree of correlation between K and Z is significant.

Ion-exchange capacity and the geometric model

The Langmuir model can provide a check on the values of P_m. The ratio of the Langmuir coefficients, a/b, is a measure of the effective exchange capacity for a given protein. These ratios at the lowest counter-ion concentrations approach the capacity of the exchanger for the protein and are compared with the P_m estimates in Table V. The two methods give reasonably good agreement considering the width of the confidence intervals. One may suspect that the large protein molecules are only adsorbing on the surface of the exchanger particles. However, through a series of void fraction experiments, Wachter[12] showed that the proteins in our system can access 57–72% of the interior of an exchanger particle, whereas NO_3^- ions can access 95%.

The geometric interaction of a charged protein surface with a charged exchanger surface has an overriding effect on Z. If the charge groups cannot orient themselves to be near each other, they cannot interact. To quantify this interaction, we have developed a geometric model of the interaction of protein charge groups with exchanger charge groups. For this model we need the average charge separation

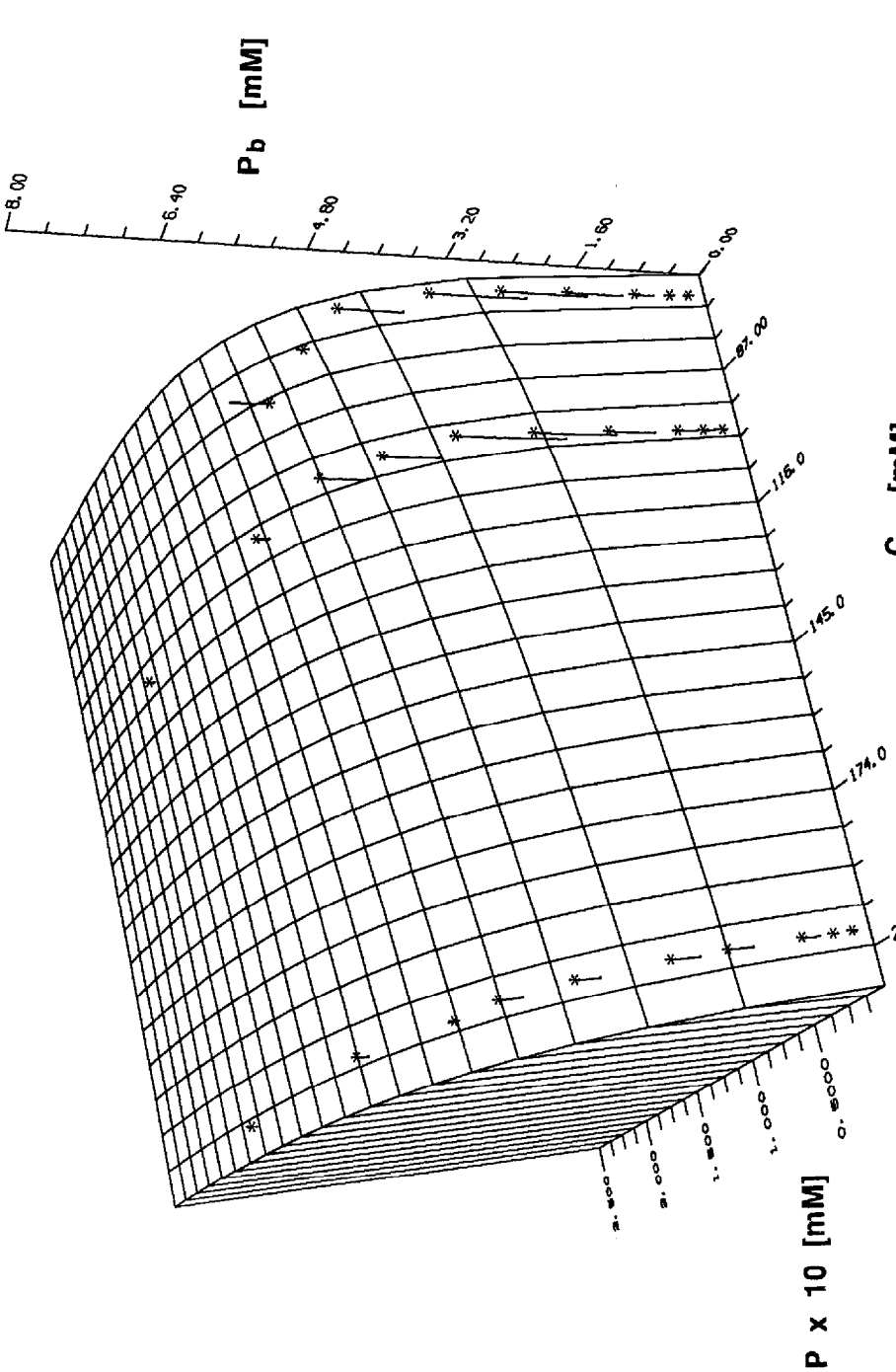

Fig. 10. Comparison of mass action model with batch data for MYO/CM/5. The vertical lines represent difference between model and data values of P_b.

TABLE IV
COMPLETE ISOTHERMS AND MODEL PARAMETERS

Conditions	*SD (mM)*	*No. of points*	*Mass action*			*Slope method*	
			K/1000	*P_m(mM)*	*Z*	*Z*	*Log K*
MYO/CM/4	1.336	26	8.92±21.76	7.98±0.22	1.36±0.69	0.6±0.082	3.8±0.087
MYO/CM/5	0.560	29	2.97±2.89	5.54±0.10	0.82±0.20	1.3±1.9	4.3±2.5
MYO/SS/5	0.527	36	8.50±8.29	7.42±0.15	1.07±0.22	1.15±1.3	4.0±1.6
LYO/CM/4	1.111	32	27.9±3.68e6	8.87±0.91	1.82±0.27	−0.15±2.1	3.4±2.2
LYO/CM/5	0.480	35	17400±34721	8.76±0.28	3.59±0.49	3.8±9.2	7.3±10.3
LYO/SS/5	0.868	35	1818±3100	10.25±0.62	2.52±0.39	2.1±7.4	5.8±7.8
BSA/DS/8	0.030	33	209.8±380.0	1.01±0.12	2.23±0.29	3.0±1.6	7.0±3.4
BSA/QS/8	0.079	28	30005±137979	1.01±0.05	2.71±0.74	3.1±10.4	8.2±21.6

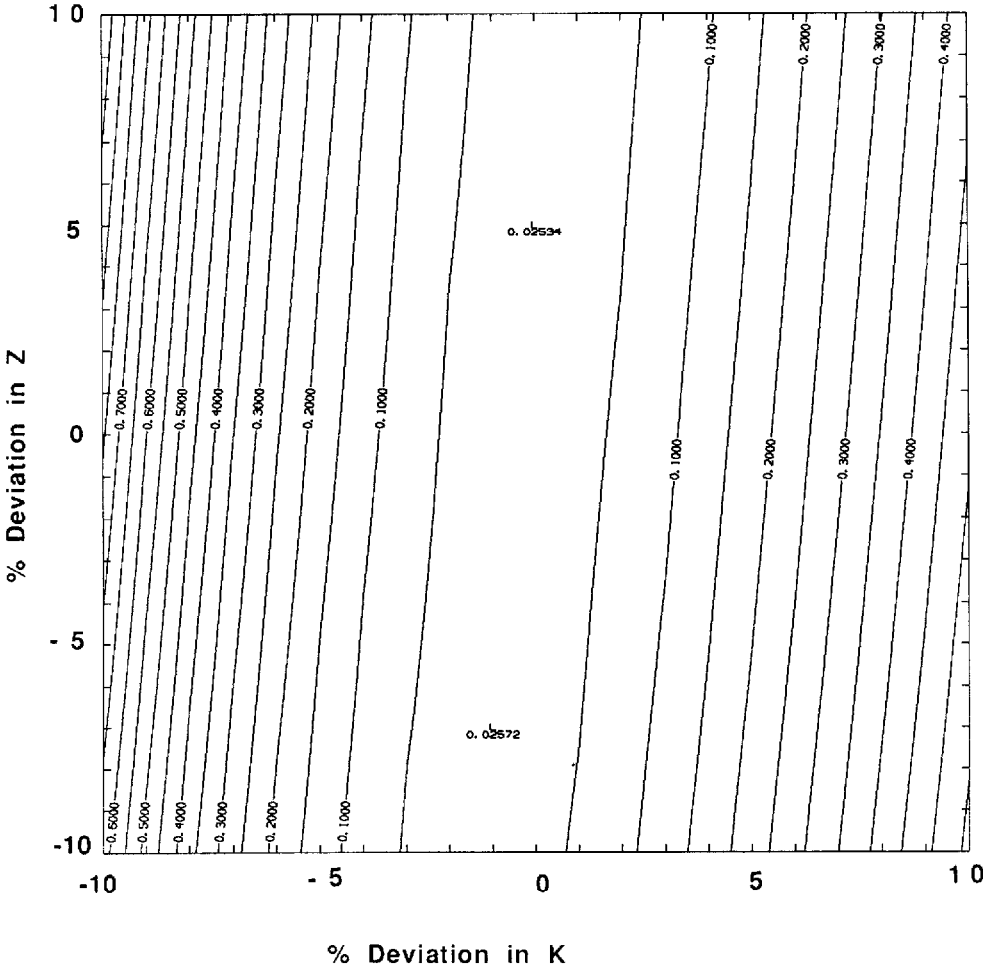

Fig. 11. SSE contours for the BSA/DS/8 isotherms with $Z=2.23$, $K=0.210 \cdot 10^6$ and $A=1.01$ mM. Span is ±10% of the parameter value.

TABLE V
COMPARISON OF PROTEIN CAPACITIES

Conditions	$P_m(mM)$	$a/b(mM)^a$	ZP_m/q_m
MYO/CM/4	8.0	7.2	0.198
MYO/CM/5	5.5	5.1	0.046
MYO/SS/5	7.4	7.9	0.038
LYO/CM/4	8.9	7.3	0.295
LYO/CM/5	8.8	6.6	0.319
LYO/SS/5	10.3	9.2	0.124
BSA/DS/8	1.2	0.58	0.027
BSA/QS/8	1.0	0.75	0.013

[a] Ratio for low salt isotherm.

distances (CSDs) for the exchangers and the overall dimensions for the proteins. Knowing the number of amino acids on the protein surface that are ionized, we made the following assumptions: (1) protein shape may be represented as a prolate spheroid and (2) excluding the void volume of 95%, the ion exchanger is a homogeneous phase in which the charges are uniformly distributed. For a large number of beads, the homogeneity will be realized. The last assumption slightly overestimates the CSD; it assumes the charges are in the 5% solid volume, but they are actually on the surface of the strands (they were determined by ion exchange with small ions). However, this error is minimal for small strands. Details of the calculations were given by Wachter[12], and the resulting numbers are shown in Table VI. The gel exchangers present an open matrix which allows even large proteins access to the interior of the beads. The "surface" seen by the protein molecules is a maze of wavy strands of varying diameters[13]. On average, the net effect is assumed to be equivalent to a flat exchanger surface with a uniform charge distribution. For the protein, we approximate the shape as an elliptical projection on to the exchanger surface.

With those approximations in place, we calculate the number of exchanger sites covered by the projection of the protein. As MYO and LYO have three different dimensions, there are two elliptical projections which represent the minimum and maximum area that the protein may cover. The corresponding numbers of sites covered for these projections are called SC_1 and SC_2, respectively. The true number of

TABLE VI
ION EXCHANGER CSDs (Å)

pH	*CM-Sepharose*	*S-Sepharose*	*DEAE-Sepharose*	*Q-Sepharose*
4.0	10.1	6.3		
5.0	8.2	6.3		
6.0			7.8	6.3
8.0			9.0	6.3

exchanger sites covered should be anywhere between the two projections. The number of sites covered by one protein is compared with the number of moles of sites covered by 1 mole of protein molecules ($f_a q_m/P_m$), where f_a is the ratio of the particle void for a protein to that for NO_3^-. The values of f_a are 0.60 (BSA), 0.73 (MYO) and 0.76 (LYO). The results of this comparison are given in Table VII. In most instances the ratio $f_a q_m/P_m$ falls near SC_1 (within experimental error). This indicates that at high loading the protein orients itself with respect to the "planar" exchanger surface such that there is a minimum of contact. Even though many exchanger sites are covered by a protein, very few are actually involved in binding with the protein. Hence the charge densities of the exchangers studied appear to be in excess of that needed to reach the average Z. This may also be seen by the lack of correlation between Z (Table IV) and the average CSD on the exchanger (Table VI) for a given protein.

Apparent binding number

The associated plots for eqn. 12 are shown in Figs. 12–14. The slopes of these lines are the limiting values of Z for low concentration (Table IV); we arrived at the estimates by linear regression. The confidence intervals on the slope and intercept, Z and K, respectively, were calculated at a 95% confidence level. There are few data points for each of these lines, as only three or four C_0 levels were covered. Consequently, the confidence intervals are fairly wide, but the fitted values of Z show reasonably good agreement with the mass action estimates of Z.

Wada and Nakamura[14] showed that most charges on a protein surface are surrounded by charges of opposite sign at neutral pH. Perutz[15] noted that most of these charges are involved in salt bridging with neighboring charges of opposite sign. The bridging reduces the tendency of the protein charge groups to bind with the charge groups on the exchanger. This could explain the low number of binding sites reported here. Similar results were obtained with amino acids by Wang *et al.*[10]. They found that

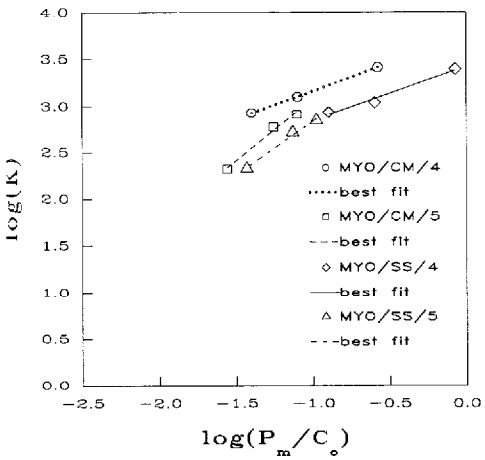

Fig. 12. Curves for slope method analysis of MYO isotherms.

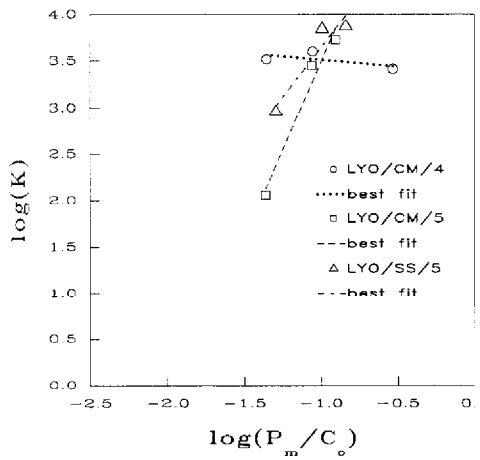

Fig. 13. Curves for slope method analysis of LYO isotherms.

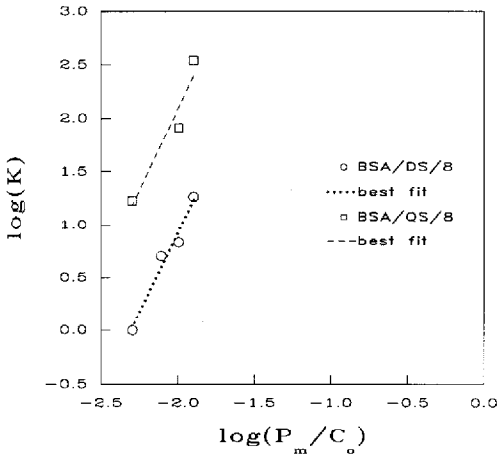

Fig. 14. Curves for slope method analysis of BSA isotherms.

when both the α-amino and α-COOH groups were ionized, bridging seemed to occur between these two nearby groups, reducing the chance of either group binding to an exchanger surface.

Since protein surface charges are due to weakly ionizable groups, the protein may carry a fractional average charge, resulting in a net fractional value for Z. Additionally, any given protein molecule may be oriented in several ways with respect to the exchanger, thus presenting different numbers of sites for ion exchange. Both of these factors contribute to the observed value of Z, which is a population-weighted average. Although the confidence intervals on the Z values in Table IV are wide enough to cover an integral number, several values of Z fall mid-way between two whole numbers. A Scatchard plot may be used to show that these fractional Z values result from two or more different binding forms of a protein in competition. Ruaan *et al.*[16] used this graphing technique for pyruvate kinase adsorbing onto a gel containing both carboxylic acid groups and Cibacron Blue F3G-A. Writing for our system and assuming one type of interaction, we have

$$\mathrm{P} + \mathrm{L} \leftrightharpoons \mathrm{P\text{–}L} \tag{14}$$

where P is the free protein, L is the exchanger site consisting of any fixed number of charge sites. The resulting Scatchard equation is

$$\frac{[\mathrm{P\text{–}L}]}{[\mathrm{P}]} = \frac{[\mathrm{L}_{\max}]}{K_\mathrm{d}} - \frac{[\mathrm{P\text{–}L}]}{K_\mathrm{d}} \tag{15}$$

where K_d is the dissociation equilibrium constant. If this relationship holds true, a plot of [P–L]/[P] *versus* [P–L] will be linear.

First, the test data set for the model was plotted in this manner. The resulting curve is concave-up, indicating negative cooperativity for the test set of parameters

($Z=4$). The Langmuir fit (which implies $Z=1$) of the test data set yielded a straight line. However, when the experimental isotherms were plotted in Scatchard form, almost all of them show a nearly exponential decay with increasing P_b (Fig. 15). This concave-up character is the result of heterogeneous binding forms in competition. The higher affinity systems showed a Gaussian-like peak (Fig. 16), which implies positive cooperative binding at low exchanger loading[17]. As the concentration increases, there is an inflection point, after which the concave-up pattern for heterogeneous binding is seen. The Langmuir model does not allow for either positive or negative cooperativity. The mass action model with $Z>1$ can account for negative-cooperative binding, but it does not allow Z to change with concentration. Hence both models give a curve that represents some average due to competing forms.

As mentioned while discussing the three-dimensional nature of the model, the protein data, in addition to previously reported data for basic amino acids[10], show that Z decreases with increasing concentration of protein or amino acid. The amino acid results and a study of cytochrome *c* by Boardman and Partridge[1] also showed that Z decreases with increasing salt concentration. In the latter work column elution volume was compared with sodium concentration. They overlaid curves predicted for various integral values of Z. At low sodium concentration (10 mM), the data followed the $Z=5$ curve, crossed over to the $Z=4$ curve as sodium concentration increased and finally approached the $Z=3$ curve at the end of their experimental conditions (Na^+ concentration = 18 mM).

Knowing that the apparent binding number is a population-weighted average of the two or more binding forms present, the task is to determine the relationship of Z to system variables. Over the course of a given separation, change in absorbed protein concentration usually has a direct effect on Z. There are two basic curve shapes proposed for this relationship: an exponential decay[10] and a decreasing sigmoidal curve[2].

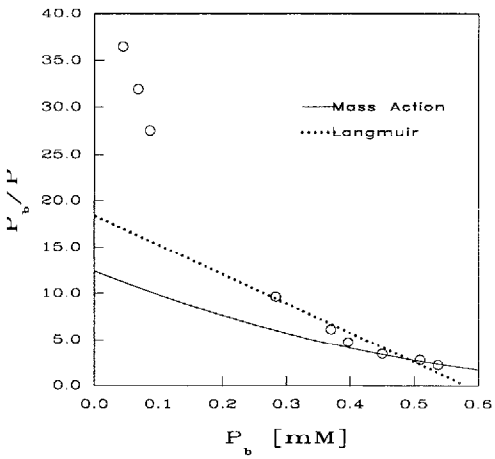

Fig. 15. Scatchard plot of BSA/DS/8 for $C_0=80$ mM, shown with best fits of Langmuir and mass action models.

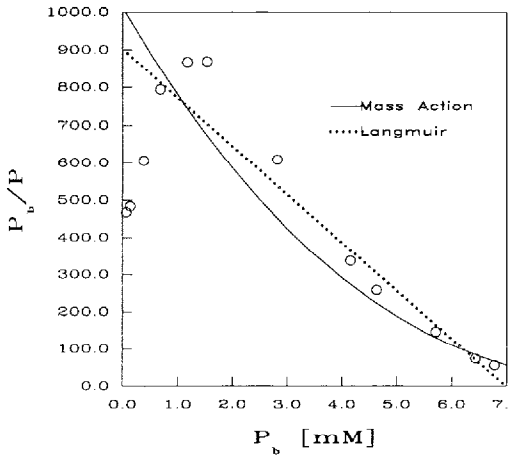

Fig. 16. Scatchard plot of LYO/SS/5 for $C_0=200$ mM, shown with best fits of Langmuir and mass action models.

TABLE VII
GEOMETRIC MODEL

Conditions	SC_1	SC_2	$f_a q_m / P_m$
MYO/CM/4	9.43	12.1	[a]
MYO/CM/5	14.3	18.4	13.0
MYO/SS/5	24.2	31.2	20.7
LYO/CM/4	6.93	10.4	4.70
LYO/CM/5	10.5	15.8	8.59
LYO/SS/5	17.8	26.7	15.6
BSA/DS/8	57.4	57.4	49.7
BSA/QS/8	117.2	117.2	124.8

[a] Insufficient data at high concentration.

The sigmoidal curve results in a total of five adjustable parameters for the proposed mass action expression. The model was applied to the set of almost linear isotherms for immunoglobulin G (IgG) on a strong anion exchanger which were reported by Mazsaroff *et al.*[2]. The counter-ion concentration ranged from 100 to 108 mM. Fitted values for Z_{min} and Z_{max} were 2.36 and 3.61, respectively. We obtained a value of 2.53 ± 0.20 for the average Z. The other two parameters, $K = 671.2 \pm 141.4$ and $P_m = 9.30 \pm 7.27$ mg, are not directly comparable to our system as the IgG bound values were in units of mass and as a different ion exchanger was used. The standard deviation for bound mass was 0.00071 mg, indicating that a three-parameter model is sufficient to describe the IgG system at the low surface coverage reported.

CONCLUSIONS

At a given pH and ionic strength, isotherms of BSA, MYO and LYO can be well described by the Langmuir equation. At a given pH and varying counter-ion concentrations, isotherms of the proteins studied can be described by mass action equilibria. The accuracy of the P_m estimation has been confirmed by comparison with the Langmuir model and with the geometric model developed in this paper. The geometric model accurately predicts a range for the molar protein capacity of an exchanger based only on exchanger CSD and overall protein dimensions. This predicted capacity agrees with mass action and Langmuir estimates. For BSA, the largest protein studied, we observed partial size exclusion from some of the interior cavities of the exchangers.

The values of Z from mass action agree with those from a slope method. These small values are supported by other work which indicates that many of the potential binding groups on a protein surface are tied up in salt bridges and that steric hindrance prevents binding of many sites. The width of the Z confidence intervals is due to Z actually being an average value over the counter-ion and protein concentration ranges studied. The mass action model describes well the equilibrium data for IgG, and the average Z determined for these data falls mid-way between the maximum and minimum Z determined by a model allowing for variation in Z (ref. 2). This indicates that what our model shows is indeed the average Z over the concentration region of interest.

In addition, plotting our isotherm data as Scatchard plot supports the claim of competition between two or more binding forms of the proteins studied. For the high-affinity systems, the Scatchard plots also showed cooperative binding at low exchanger loading. Even though the Langmuir and mass action models give close fits of the isotherm data, the Scatchard plots clearly show that they really represent the average behavior.

ACKNOWLEDGEMENTS

The authors thank Professor R. E. Eckert for consultations on statistical analysis of the data and J. Berninger for coding parts of the computer programs. This research was supported by NSF grants CBT 8412013, CBT 8620221 and ECE 8613167.

SYMBOLS AND ABBREVIATIONS

a, b	Langmuir coefficients
BSA	bovine serum albumin
C	salt counter-ion concentration in the bulk phase
C_b	salt counter-ion concentration in the adsorbed phase
C_0	initial salt concentration in the bulk phase
CSD	charge separation distance (Å)
$F_{0.05}(n,m)$	F statistic, n parameters, m degrees of freedom
f_a	ratio of particle void for a protein over particle void for NO_3^-
k_d	dissociation equilibrium constant
K	mass action constant
K_b	binding constant
K_f	fractional accessibility coefficient
L	exchanger binding site (any number of charge sites)
L_{max}	maximum number of exchanger binding sites
LYO	lysozyme
MYO	myoglobin
P	protein concentration in the bulk phase (mM)
P_b	protein concentration adsorbed on the exchanger [mmol protein per liter of exchanger (packed bed volume)]
$\hat{P}_b$	model prediction of P_b
P_m	protein capacity of the ion exchanger [mmol protein per liter of exchanger (packed bed volume)]
P–L	protein–exchanger binding complex concentration
q_m	small ion capacity of an exchanger [mequiv. ion per liter of exchanger (packed bed volume)]
S_c	sum of squares error for a contour
S_{min}	minimum sum of squares from least-squares regression
SD	standard deviation
s_{pool}	pooled standard deviation (mM)
SSE	sum of squares of error
Z	average number of binding sites per molecule

REFERENCES

1 N. K. Boardman and S. M. Partridge, *Biochem. J.*, 59 (1955) 543.
2 I. Mazsaroff, S. Cook and F. E. Regnier, *J. Chromatogr.*, in press.
3 H. F. Walton, in E. Heftmann (Editor), *Chromatography*, Van Nostrand Reinhold, New York, 1975, Ch. 12, p. 312.
4 A. Velayudhan and Cs. Horváth, *J. Chromatogr.*, 367 (1986) 160.
5 W. Kopaciewicz, M. A. Rounds, J. Fausnaugh and F. E. Regnier, *J. Chromatogr.*, 266 (1983) 3.
6 M. A. Rounds and F. E. Regnier, *J. Chromatogr.*, 283 (1984) 37.
7 F. E. Regnier and I. Mazsaroff, *Biotechnol. Progress*, 3 (1987) 22.
8 N.-H. L. Wang, in J. A. Asenjo (Editor), *Downstream Processing in Biotechnology*, Marcel Dekker, New York, 1989, in press.
9 Pharmacia Fine Chemicals, *Ion Exchange Chromatography: Principles and Methods*, Pharmacia, Uppsala, Sweden, 1983.
10 N.-H. L. Wang, Q. Yu. and S. U. Kim, *React. Polym. Ion Exch. Sorbents*, (1989) in press.
11 G. E. P. Box and W. G. Hunter, *Technometrics*, 4 (1962) 301.
12 R. O. Wachter, *M.S. Thesis*, Purdue University, 1987.
13 S. Arnott, A. Fulmer, W. E. Scott, I. C. M. Dea, R. Moorhouse and D. A. Rees, *J. Mol. Biol.*, 90 (1974) 269.
14 A. Wada and H. Nakamura, *Nature (London)*, 293 (1981) 757.
15 M. F. Perutz, *Science*, 201 (1978) 1187.
16 R.-C. Ruaan, J. B. Blair and J. A. Shaeiwitz, *Biotechnol. Progress*, 4 (1988) 107.
17 J. D. Andrade, in J. D. Andrade (Editor), *Surface and Interfacial Aspects of Biomedical Polymers, Vol 2, Protein Adsorption*, Plenum Press, New York, 1985, Ch. 1, p. 1.
18 P. G. Righetti and T. Caravaggio, *J. Chromatogr.*, 127 (1976) 1.